

# First principle investigation of the structural and electronic properties of the gallium clusters and their influence on the melting characteristics

Sailaja Krishnamurty, Kavita Joshi, Shahab Zorriasatein, and D. G. Kanhere  
*Department of Physics, and Centre for Modeling and Simulation,  
University of Pune, Ganeshkhind, Pune-411 007, India*

## Abstract

First principle calculations have been performed to understand the experimentally observed size sensitive variations in the characteristics of heat capacities of gallium clusters [G. A. Breaux *et al.* J. Am. Chem. Soc., **126**, 8628 (2004)]. It was reported that while some clusters exhibit a clear solid like to liquid like transition others exhibit a continuous transition with no peak in the heat capacity curve. In addition, the clusters also exhibit a variation of about 300 K (500–800 K) in the melting temperature across the size range of 20 to 46. In the present work we correlate the observed finite temperature properties to its geometry and nature of bonding in the ground state. We demonstrate that the local order (i.e., island of atoms bonded with similar strength) in the ground state geometry is responsible for the variation in the shape of the heat capacity curve. We attribute the higher melting temperature of clusters to the presence of distinct core and strong covalent bonds between the core and surface atoms.

PACS numbers: 61.46.Bc, 36.40.Mr, 36.40.–c, 36.40.Cg

## I. INTRODUCTION

During the past decade or so, a number of systematic calorimetric measurements probing the finite temperature behavior of unsupported free clusters have yielded unexpected and rich physics.<sup>1,2,3,4</sup> One of the first reports is on the measurement of melting temperatures ( $T_m$ ) of simple metal clusters of sodium in the size range of 55 to 357 atoms.<sup>1</sup> The measured melting temperatures were found to be an irregular function of the cluster sizes with melting peaks showing no clear correlations with the observed magic numbers in sodium.<sup>2</sup> The second measurement was reported by Jarrold and co-workers which brought out additional important aspects in the melting of finite size clusters.<sup>3,4</sup> The systems investigated are free clusters of gallium in the size range of 30 to 55.<sup>4</sup> The measured heat capacities of the clusters in the above range revealed three very interesting features: (1) Higher than bulk melting temperatures ( $T_{m[bulk]} = 303$  K) in all the clusters (also seen in two smaller clusters viz., Ga<sub>17</sub> and Ga<sub>20</sub>) in direct contradiction with the accepted paradigm, *viz.*, the reduction in the melting temperatures with the size.<sup>3</sup> (2) The size sensitive behavior of the shape of the heat capacities where addition of even one atom results in a dramatic change of shape, prompting some of the clusters to be called as “Magic Melters”.<sup>4</sup> This means that while some clusters do undergo a conventional and clear melting transition, others undergo a near continuous transition making it very difficult to identify any meaningful transition temperature. (3) A variation of about 300 K (500–800 K) in the  $T_m$  across the sizes between 20 to 46. For example, Ga<sub>20</sub>, Ga<sub>46</sub>, and Ga<sub>47</sub> exhibit a highest melting temperature of about 800 K while the intermediate clusters such as Ga<sub>31</sub>, Ga<sub>33</sub>, Ga<sub>37</sub>, Ga<sub>41</sub>, etc., exhibit a lower melting temperature of the order of 500–600 K. Thus, the size sensitive variations in melting temperature are not monotonic in nature. Such variations in the melting temperature of clusters are also observed experimentally in the case of aluminum clusters.<sup>5</sup>

An explanation and understanding of some of the unexpected and puzzling experimental observations noted above warranted detailed ab initio Molecular Dynamical (MD) simulations based on Density Functional Theory (DFT). A clear signal for needing such an approach came from detailed investigations using classical inter atomic potentials, which failed to reproduce the data on sodium, even qualitatively.<sup>6</sup> On the other hand, even early DFT based investigations, limited to short simulation times, were successful in providing some insights into the phenomena of melting.<sup>7</sup> Recently, works of Chacko et. al.,<sup>8</sup> and Aguado and Lopez<sup>9</sup>

over the entire size range have reported excellent agreement with the experimental melting temperatures of these clusters. These calculations indicate that the geometry plays a more direct and significant role with the electronic structure influencing it in a more subtle way. Indeed it must be emphasized that the nature of bonding and the energetics turn out to be two crucial ingredients, making an explicit quantum mechanical treatment of electrons mandatory.

In two short communications, we have addressed the issues of higher than bulk melting point<sup>10</sup> and size sensitive nature observed in gallium clusters.<sup>11</sup> The predominantly covalent nature of bonding in the gallium clusters in contrast with predominant metallic bonding in bulk-Ga has been shown to be responsible for the higher than bulk melting point of clusters. These reports are limited to Ga<sub>13</sub> and Ga<sub>17</sub> which was later on extended to Ga<sub>30</sub> and Ga<sub>31</sub>. By examining the geometry and the finite temperature behavior of Ga<sub>30</sub> and Ga<sub>31</sub>, the pair displaying maximum size sensitivity, we explained that the dramatic change in their heat capacities has geometric origin.<sup>11</sup> Specifically we established a direct correlation between the nature of the ground state and the observed heat capacity. An “ordered” cluster is expected to display a well characterized melting transition showing an identifiable, albeit broad peak. On the other hand a completely “disordered” cluster will undergo a continuous transition with a very broad heat capacity. Quite clearly such a description is qualitative and needs further quantifications. It also raises questions about the universality of such a phenomenon. The earlier work is based on two specific clusters, viz., Ga<sub>30</sub> and Ga<sub>31</sub> (as well as Ga<sub>17</sub> and Ga<sub>20</sub>)<sup>12</sup> where such an effect was discussed and did not address the issue of observed systematic behavior over entire range and the shift in  $T_m$  to higher value in case of Ga<sub>20</sub> and Ga<sub>46</sub>.

The present work is an attempt to understand and evolve a complete picture of the experimental observations over the reported size range. Evidently, complete thermodynamic calculations based on an ab initio MD are prohibitively expensive. However, our earlier work clearly brings out the two main ingredients which are essential and perhaps sufficient for such an understanding, namely the analysis of ground state geometry and the nature of bonding in the clusters. In the present work, we have carried out such an analysis for the gallium clusters in the size range of 20 to 55. It may be mentioned that many of the geometries do not display any obvious rotational symmetry. This is especially true of large clusters. Therefore, it is not straightforward to characterize the nature of order

and disorder using some quantitative measure. In this sense the situation is some what unsatisfactory. However, considerable insight can be gained by analyzing the shape of the cluster, distribution of shortest bond lengths (in other words strongest covalent bonds) and pair correlation function. Another extremely useful quantity is the Electron Localization Function (ELF) which provides a semi quantitative picture of the nature of bonding and the connectivity of atoms. In view of the fact that we have made use of ELF extensively, this function will be discussed in detail later.

It is most profitable to put the present work on gallium clusters in the context of known structural trends in small gallium clusters and bulk properties. The evolutionary trends in the geometries of small clusters ( $N \leq 26$ ) have been investigated by Song and Cao.<sup>13</sup> In smaller clusters it is relatively easy to discern the symmetry. For example, the ground state geometry of  $\text{Ga}_{13}$  is decahedron. The next two structures in size are obtained by capping one of the square faces by one and two atoms, respectively. This distorts the structure and disturbs the symmetry. By the time four atoms are added, viz.,  $\text{Ga}_{17}$ , the structure is completely distorted. This evolutionary trend changes after  $\text{Ga}_{17}$  and a structure with identifiable ordered planes develops e.g., as seen in  $\text{Ga}_{20}$ . Such an evolutionary trend in the geometries from well ordered one like  $\text{Ga}_{13}$  to another partially ordered one like  $\text{Ga}_{20}$  through a disordered one like  $\text{Ga}_{17}$  is responsible for the size sensitive nature. Since there is nothing specific about gallium per se, in so far as the evolutionary trends are concerned, the size sensitive nature of the heat capacity should be an universal phenomenon. Indeed, our calculation on clusters of  $\text{Na}_n$  ( $n= 55$  and  $58$ ),<sup>14</sup>  $\text{Au}_n$  ( $n=19$  and  $20$ ),<sup>15</sup> and smaller clusters of  $\text{Ga}_n$  ( $n=17$  and  $20$ )<sup>12</sup> supports this conjecture. In light of the above discussion, the availability of experimental heat capacity data on gallium for all the sizes within a given range presents an interesting opportunity to carry out detailed investigations of their ground state properties.

In the bulk phase, gallium has been described as a metallic molecular solid. Gong et. al.,<sup>16</sup> have calculated the band structure of  $\alpha$ -Ga and have shown that molecular character and metallic conduction coexist.  $\alpha$ -Ga is a face centered orthorhombic solid with 8 atoms in the cubic unit cell. It has only one nearest neighbor at a distance of 2.44 Å. The next three shells contain two atoms each at distances of 2.71 Å, 2.74 Å, and 2.83 Å, respectively. The structure can be regarded as strongly buckled planes connected by the shortest bonds. Fig. 1 shows the atomic arrangement from this perspective. The short bonds across the planes

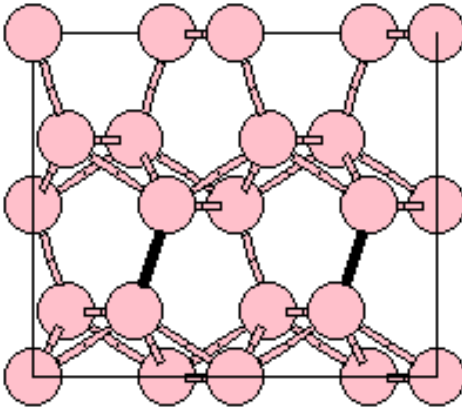


FIG. 1: Unit cell of  $\alpha$ -Ga. It shows two buckled planes. The dark line joining the atoms corresponds to the inter planar covalent bond discussed in the text.

(dark lines in Fig. 1) show covalent character, while the in plane electrons are delocalized. The density of states show a pseudo gap attributed to the covalent band. Interestingly, the parent structure called as Ga-II is a distorted tetragonal face centered cubic (FCC), which can be obtained under pressure of 35 kbar. This structure is quite close in energy to the  $\alpha$ -Ga and is metallic. In other words Ga-II, the metallic FCC structure rearranges into  $\alpha$ -Ga, once the pressure is released forming a covalent bond. Thus, the tendency to form a covalent bond is already there in a nascent form and given a chance to further rearrange the atomic positions, as is the case in clusters, the structure may prefer to form covalent bonds. This is what we observe in the finite sizes of  $\text{Ga}_n$  clusters where,  $n \approx 55$ . In fact, our detailed analysis of the ground state geometries of  $\text{Ga}_n$  ( $n= 13-55$ ) clusters shows an interesting pattern as to how the covalent bonds in the cluster rearrange themselves, leading to significant variations in the melting temperature. At what sizes the partial metallic bonds are formed is an interesting question but beyond the scope of this work.

In what follows, we study the ground state geometries of selected gallium clusters (viz.,  $\text{Ga}_n$ ,  $n= 13, 17, 20, 30, 31, 33, 37, 46$ , and  $55$ ) and discern the evolutionary trends. Along with the evolutionary trends, we also analyze the nature of bonding, the number of covalent bonds, and their distribution within the clusters. Using these trends, we bring out the factors contributing to the non-monotonic variations in the melting temperature. Thus, we expect our current work to throw light on general experimental observations over the reported size range.

## II. COMPUTATIONAL DETAILS

In order to have a realistic guess for the ground state, we have optimized about 300 geometries for each of these clusters. The initial configurations for the optimization were obtained by carrying out a constant temperature dynamics of 100 ps each at various temperatures between 600 to 1200 K. The optimization was carried out using Vanderbilt's ultra soft pseudo potentials<sup>17</sup> within the Generalized Gradient Approximation (GGA) for describing the core-valance interactions as implemented in the VASP package.<sup>18</sup> For all the calculations, we take the  $4s^2$  and  $4p^1$  electrons as valence electrons and the  $3d$  electrons as a part of the ionic core. An energy cutoff of about 9.54 Ry is used for the plane wave expansion of the wave function, with a convergence in the total energy of the order of 0.0001 eV.

Once the ground state geometry is obtained from the first principles calculations, various structural and electronic properties of the cluster in its ground state were analyzed. The structural properties analyzed are (i) bond length variations within the cluster, (ii) distance from Centre of Mass (COM), and (iii) shape of the cluster. The shape of the cluster is quantified using the deformation coefficient ( $\epsilon_{\text{pro}}$ ). For a given configuration,  $\epsilon_{\text{pro}}$  is defined as

$$\epsilon_{\text{pro}} = \frac{2Q_z}{Q_x + Q_y} \quad (1)$$

where,  $Q_x$ ,  $Q_y$  and  $Q_z$  are the eigenvalues, in ascending order of the quadrapole tensor

$$Q_{ij} = \sum_I R_{Ii} R_{Ij} \quad (2)$$

$I$  runs over the number of ions and  $R_{Ii}$  is the  $i$ th coordinate ( $i$  and  $j$  run from 1 to 3) of the ion ' $I$ ' relative to the center of mass of the cluster. In simple terms,  $Q_x$ ,  $Q_y$ , and  $Q_z$  define the spread of the cluster along the X, Y, and Z axis. Thus, configuration with spherical shape has eigen values  $Q_x \approx Q_y \approx Q_z$  ( $\epsilon_{\text{pro}}=1$ ). A prolate configuration has  $Q_z \gg Q_y \approx Q_x$ , while a structure with oblate configuration has  $Q_z \approx Q_y \gg Q_x$ .

The nature of bonding between the atoms in a cluster is analyzed using Electron Localization Function (ELF).<sup>19,21</sup> For a single determinantal wave function built from Kohn-Sham orbitals,  $\psi_i$ , the ELF is defined as,<sup>22</sup>

$$\chi_{\text{ELF}} = [1 + (D/D_h)^2]^{-1}, \quad (3)$$

where

$$D_h = (3/10)(3\pi^2)^{5/3} \rho^{5/3}, \quad (4)$$

$$D = (1/2) \sum_i |\nabla\psi_i|^2 - (1/8)|\nabla\rho|^2/\rho, \quad (5)$$

with  $\rho \equiv \rho(\mathbf{r})$  being the valence electron density.  $D$  is the excess local kinetic energy density due to Pauli repulsion and  $D_h$  is the Thomas–Fermi kinetic energy density. The numerical values of  $\chi_{\text{ELF}}$  are conveniently normalized to a value between zero and unity. A value of 1 represents a perfect localization of the valence charge while the value for the uniform electron gas is 0.5. Typically, the existence of an isosurface in the bonding region between two atoms at a high value of  $\chi_{\text{ELF}}$  say,  $\geq 0.70$ , signifies a localized bond in that region.

Recently, Silvi and Savin<sup>19</sup> introduced a nomenclature for the topological connectivity of the ELF. According to this description, the molecular space is partitioned into regions or basins of localized electron pairs. At very low values of ELF all the basins are connected (disynaptic basins). In other words, there is a single basin containing all the atoms. As the value of  $\chi_{\text{ELF}}$  is increased, the basins begin to split, and finally we will have as many basins as the number of atoms. The value of ELF at which the basins split (a disynaptic basin splits into two monosynaptic basins) is a measure of the interaction between the different basins (a measure of the electron delocalization).

### III. RESULTS AND DISCUSSION

In order to gain some insight into the experimentally observed differences in the heat capacity curves of  $\text{Ga}_n$  ( $n = 17 - 55$ ), we have investigated the ground state geometries of selected clusters, viz.,  $\text{Ga}_n$ ,  $n = 13, 17, 20, 30, 31, 33, 37, 40, 44, 46, 55$  and analyzed the differences in their structure and bonding. The choice of these clusters is dictated so as to represent the changing nature of the heat capacities across the measured series. For example, among these clusters,  $\text{Ga}_{17}$ ,  $\text{Ga}_{30}$ , and  $\text{Ga}_{55}$  have very broad heat capacities.  $\text{Ga}_{40}$  and  $\text{Ga}_{44}$  show a weak peak around 550 K and 700 K, respectively.  $\text{Ga}_{20}$ ,  $\text{Ga}_{31}$ ,  $\text{Ga}_{33}$ ,  $\text{Ga}_{37}$ , and  $\text{Ga}_{46}$  have a well recognized peak. Among these,  $\text{Ga}_{20}$  and  $\text{Ga}_{46}$  melt around 800 K, while  $\text{Ga}_{31}$ ,  $\text{Ga}_{33}$ , and  $\text{Ga}_{37}$  melt between 550–600 K.  $\text{Ga}_{13}$  is taken as a reference cluster to analyze the growth pattern in these clusters.

In Fig. 2, we show the ground state geometry of these clusters obtained in our search. The atoms shown in light color (blue on line) indicate the growth of the cluster over the previous one. The shape of these clusters is analyzed using  $\epsilon_{\text{pro}}$  and eigen values of quadrapole tensor

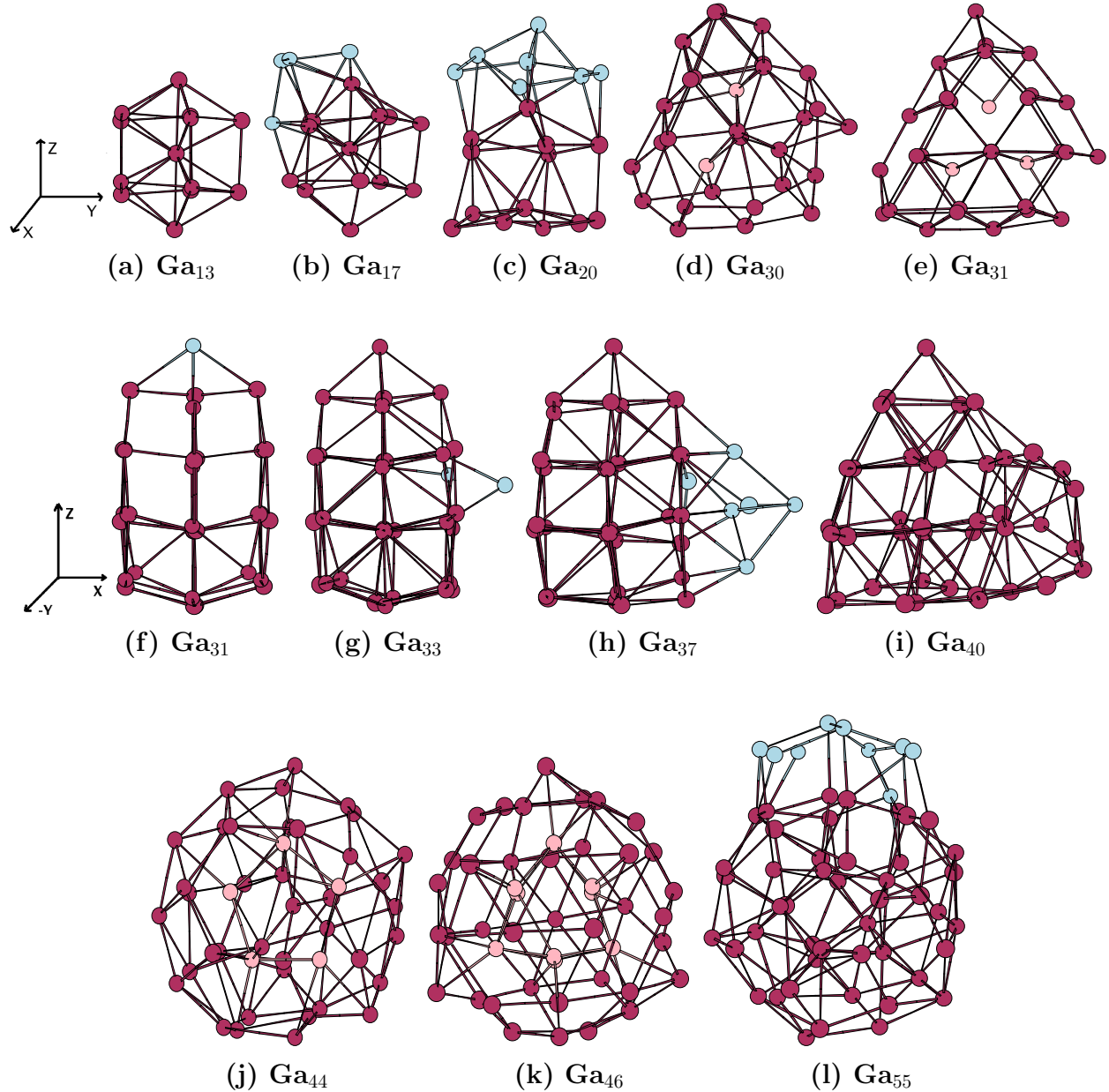


FIG. 2: Ground state geometries of selected gallium clusters between  $\text{Ga}_{13}$  and  $\text{Ga}_{55}$

which are shown in Fig. 3 and Fig. 4, respectively. We begin our discussion with a note on  $\text{Ga}_{13}$  shown in Fig. 2–(a). The ground state geometry of  $\text{Ga}_{13}$  was found to be slightly distorted decahedron in previous works.<sup>10,13,20</sup> The cluster is nearly spherical in shape with  $\epsilon_{pro} \approx 1.1$ . The inter-planar and core-surface bonds are the shortest ones (2.43–2.65 Å) in the cluster. The intra-planar bond distances are the longer ones and vary between 2.85–3.00 Å. Addition of 4 atoms to  $\text{Ga}_{13}$  results in a deformation of decahedron as seen from Fig. 2–(b). The atoms shown in red (dark color) indicate the deformed structure of  $\text{Ga}_{13}$ ,

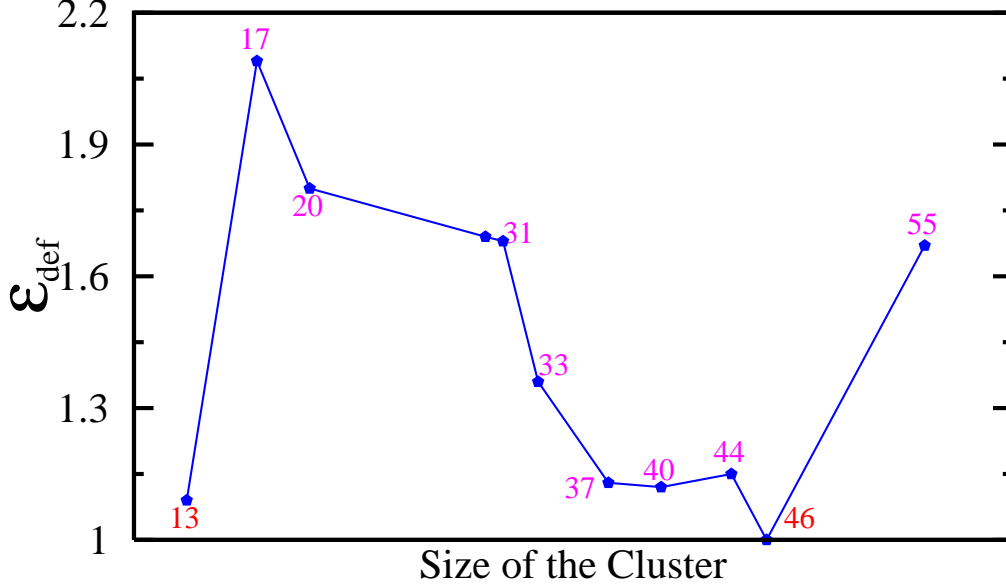


FIG. 3: Deformation co-efficient parameter ( $\epsilon_{pro}$ ) of various gallium clusters.

while the atoms in blue (light color) show the extra four atoms. It is clearly seen from this figure as well as from the analysis of  $Q_x$ ,  $Q_y$ , and  $Q_z$  (see Fig. 4) that  $\text{Ga}_{17}$  is a growth over  $\text{Ga}_{13}$  along  $Z$ -axis. The  $\epsilon_{pro}$  of  $\text{Ga}_{17}$  is  $\approx 2.1$ . The shortest bonds (2.50–2.70 Å) in  $\text{Ga}_{17}$  are randomly distributed (scattered) within the cluster unlike in case of  $\text{Ga}_{13}$ , where they are localized. The implication of this distribution of shortest bonds is brought out more clearly in the later section where we discuss their connectivity and its relation with the melting temperature.

Fig. 2-(c) shows the ground state geometry of  $\text{Ga}_{20}$ . The atoms in light color (blue on line) are the extra seven atoms that form a dome like structure on the deformed  $\text{Ga}_{13}$  cluster. The cap to the top plane of  $\text{Ga}_{13}$  now becomes the core atom in case of the  $\text{Ga}_{20}$ . Thus,  $\text{Ga}_{20}$  is also obtained by addition of atoms on deformed  $\text{Ga}_{13}$  along the  $Z$ -axis. The eigen values of quadrupole tensor and  $\epsilon_{pro}$  ( $\approx 1.8$ ) clearly indicate  $\text{Ga}_{20}$  to be prolate in shape. As in case of  $\text{Ga}_{13}$  and  $\text{Ga}_{17}$ , the atoms are bonded to each other through bond lengths ranging between 2.54–3.00 Å. A careful examination of the distribution of bond lengths in  $\text{Ga}_{20}$  cluster reveals that the shortest bond lengths (2.54–2.62 Å) in the cluster are localized

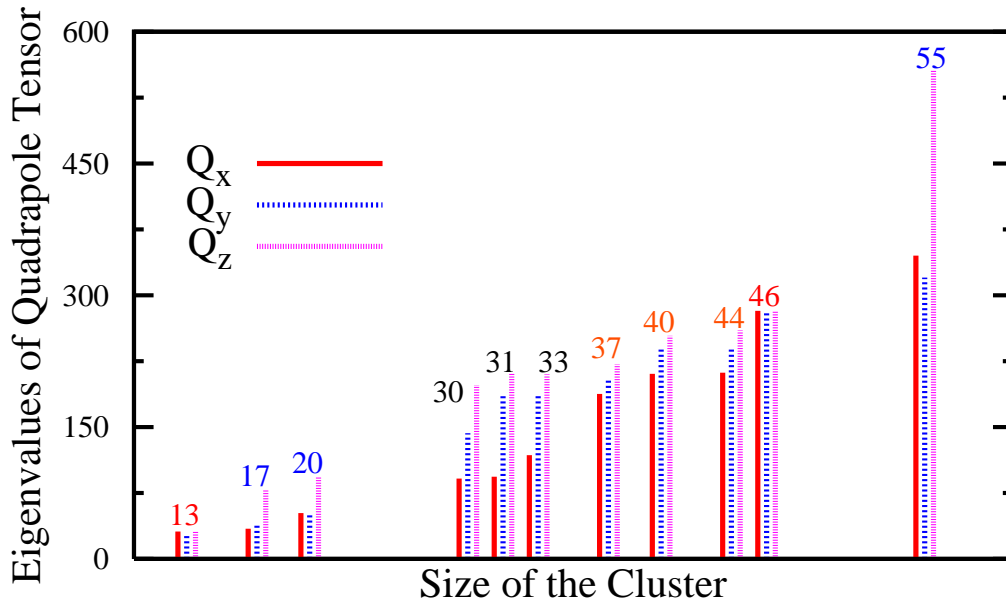


FIG. 4: Eigen values of the quadrupole tensor for gallium clusters.

in the newly added (top) and bottom planes of the cluster. The core atom of the cluster is connected to the surface atoms with bond lengths of 2.65–2.70 Å, while rest of the atoms within the cluster are connected to each other through varying lengths of 2.73–3.00 Å.

Addition of 10 atoms to  $\text{Ga}_{20}$ , viz.,  $\text{Ga}_{30}$ , results in a configuration with stacked planes as shown in Fig. 2–(d). The  $Q_x$ ,  $Q_y$ , and  $Q_z$  values show that the growth is predominantly along the Y and Z-axis resulting in a nearly oblate configuration.  $\text{Ga}_{30}$  does not have a distinct core. However, it has two interstitial atoms (atoms not facing the surface) connected to each other and to the surface atoms through bond lengths of  $\approx 3.0$  Å (shown in light red color on line). The shortest bonds are randomly distributed within the cluster. Addition of one atom to  $\text{Ga}_{30}$  results in a significant reordering of the planes and symmetric distribution of atoms in the cluster (cluster has  $C_{2v}$  symmetry) as seen from Fig. 2–(e) (for a detailed discussion on  $\text{Ga}_{30}$  and  $\text{Ga}_{31}$  see Ref. 11). Another perspective of  $\text{Ga}_{31}$  (Fig. 2–(f)) and  $Q_x$ ,  $Q_y$ , and  $Q_z$  values clearly show the cluster to be oblate in shape.  $\text{Ga}_{31}$  also does not have a distinct core. It has three interstitial atoms (shown in light red color on line) which are weakly bonded (distances  $\geq 2.90$  Å) to each other as well as to surface atoms. The shortest bonds in the

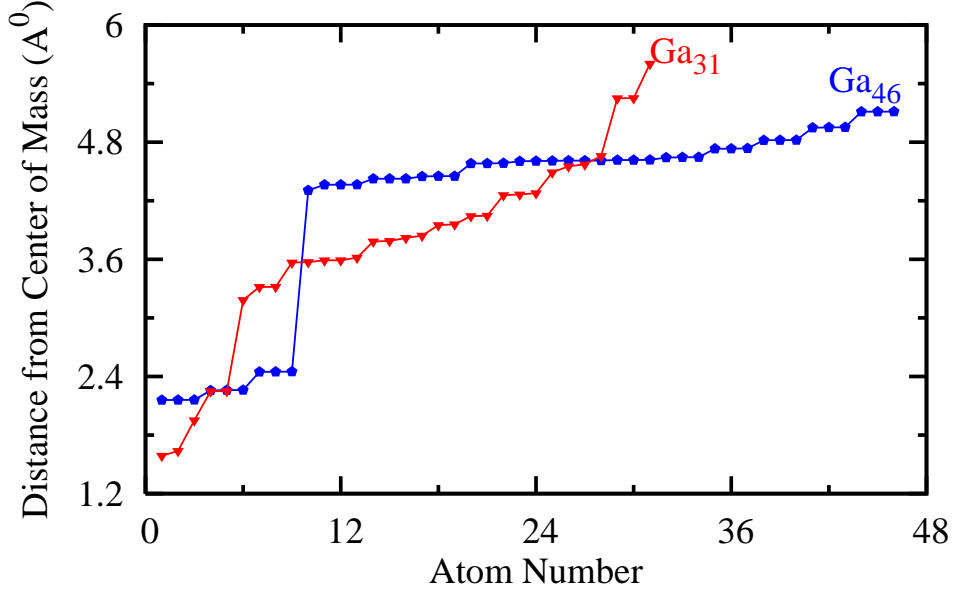


FIG. 5: Distance of atoms from Centre of Mass (COM) in  $\text{Ga}_{31}$  and  $\text{Ga}_{46}$  clusters.

cluster are localized within the same plane. Fig. 2-(g) shows  $\text{Ga}_{33}$  along the X-Z plane. We note that while  $\text{Ga}_{33}$  remains identical to  $\text{Ga}_{31}$  along the Y-Z plane (figure not shown), what is visibly different is the presence of an extra protruding atom along the X-axis. This growth continues in  $\text{Ga}_{37}$  as seen from its ground state geometry in Fig. 2-(h). This growth is also evident from the increasing values of  $Q_x$  and a sudden decrease in the  $\epsilon_{\text{pro}}$ . Both  $\text{Ga}_{33}$  and  $\text{Ga}_{37}$  retain the stacked planes configuration similar to  $\text{Ga}_{30}$  and  $\text{Ga}_{31}$ . The planes are well defined in both the cases and the clusters do not have a distinct core. The clusters continue to grow along the the X-axis as seen in the ground state geometry of  $\text{Ga}_{40}$  (shown along the X-Z plane) in Fig. 2-(i). Addition of four more atoms to  $\text{Ga}_{40}$ , however, leads to a significant rearrangement of atoms within the cluster with out any preferential growth along any axis resulting in a nearly spherical structure of  $\text{Ga}_{44}$  (shown in Fig. 2-(j)) with  $\epsilon_p \approx 1.1$ . We note that as the cluster evolves into a spherical shape as in case of  $\text{Ga}_{44}$ , we once again note the presence of a distinct core shell.  $\text{Ga}_{44}$  has five core atoms (shown in light red color on line). Addition of 2 atoms to  $\text{Ga}_{44}$  results in a highly symmetrical cluster ( $C_{3v}$  symmetry) with 9 core atoms and a spherical configuration ( $\text{Ga}_{46}$  shown in Fig. 2-(k)) with  $\epsilon_p \approx 1.0$ . To summarize, the clusters undergo a spherical to prolate transition ( $\text{Ga}_{13}$ - $\text{Ga}_{20}$ ) followed by a prolate to oblate transition ( $\text{Ga}_{20}$ - $\text{Ga}_{31}$ ) and an oblate to spherical transition

(Ga<sub>31</sub>–Ga<sub>46</sub>). As the clusters grow further, it is seen that the atoms begin to accumulate once again preferentially along one axis, leading to prolate configurations as seen in Ga<sub>55</sub> (Fig. 2–(1)). We predict here that the clusters are likely to undergo once again a prolate to oblate and an oblate to spherical transition as the number of atoms continue to increase. In the studied size range we notice that the clusters with spherical configurations have distinct core, while the clusters with oblate configurations do not have any core. This is clearly seen from Fig. 5, in which we show the distance of atoms from the COM of Ga<sub>31</sub> which is oblate in shape and Ga<sub>46</sub>, a spherical structure. Ga<sub>46</sub> has a clear shell structure, while Ga<sub>31</sub> does not have a distinct core but is characterized by interstitial atoms.

To understand the reasons behind the occurrence of so called “melters” and “non–melters”, we analyze the nature of bonding in the clusters studied. In Fig. 6, we show the isosurface of ELF at a value of  $\chi_{\text{ELF}} = 0.70$  for all the clusters. The black lines join the atoms in the same basin. A careful examination of the basin structures reveals an interesting contrast between “non–melters” (Ga<sub>n</sub>, n= 17, 30, 40, 44, and 55) and “melters” (Ga<sub>n</sub>, n=20, 31, and 37). The “non–melters” show a fragmented pattern of basins. In other words, there are many basins each consisting of not more that 4–5 atoms. In contrast, “melters” have at least one large basin consisting of 10 atoms or more. Ga<sub>46</sub>, a “melter”, apparently appears to have fragmented basin as seen visually. A detailed examination reveals that all the 9 core atoms are connected at the value of  $\chi_{\text{ELF}} = 0.70$  forming a single basin (indicated by an arrow). We further note that these core atoms are also connected to the surface atoms, there by forming a single large basin of 15 atoms. This is made more clear in the next section where we show the schematic representation of the covalent bonds in each cluster.

To summarize, the clusters exhibiting a sharp solid–liquid transition are seen to have substantial number of atoms connected through a single basin. Thus, a large group of atoms are bonded together with a similar strength forming an island of local order and therefore it is reasonable to expect that they will ‘melt’ together. In this sense the cluster can be considered as (at least partially) ordered and will show a well defined peak in the heat capacity. On the contrary, in clusters exhibiting broad or continuous solid–liquid transition, each atom (possibly a group of atoms) has different local environment. That means different atoms are bonded with the rest of the system with varying strength. Consequently, their dynamical behavior as a response to temperature will differ. Some of the atoms pickup kinetic energy at low temperatures, while the others may do so at higher temperatures.

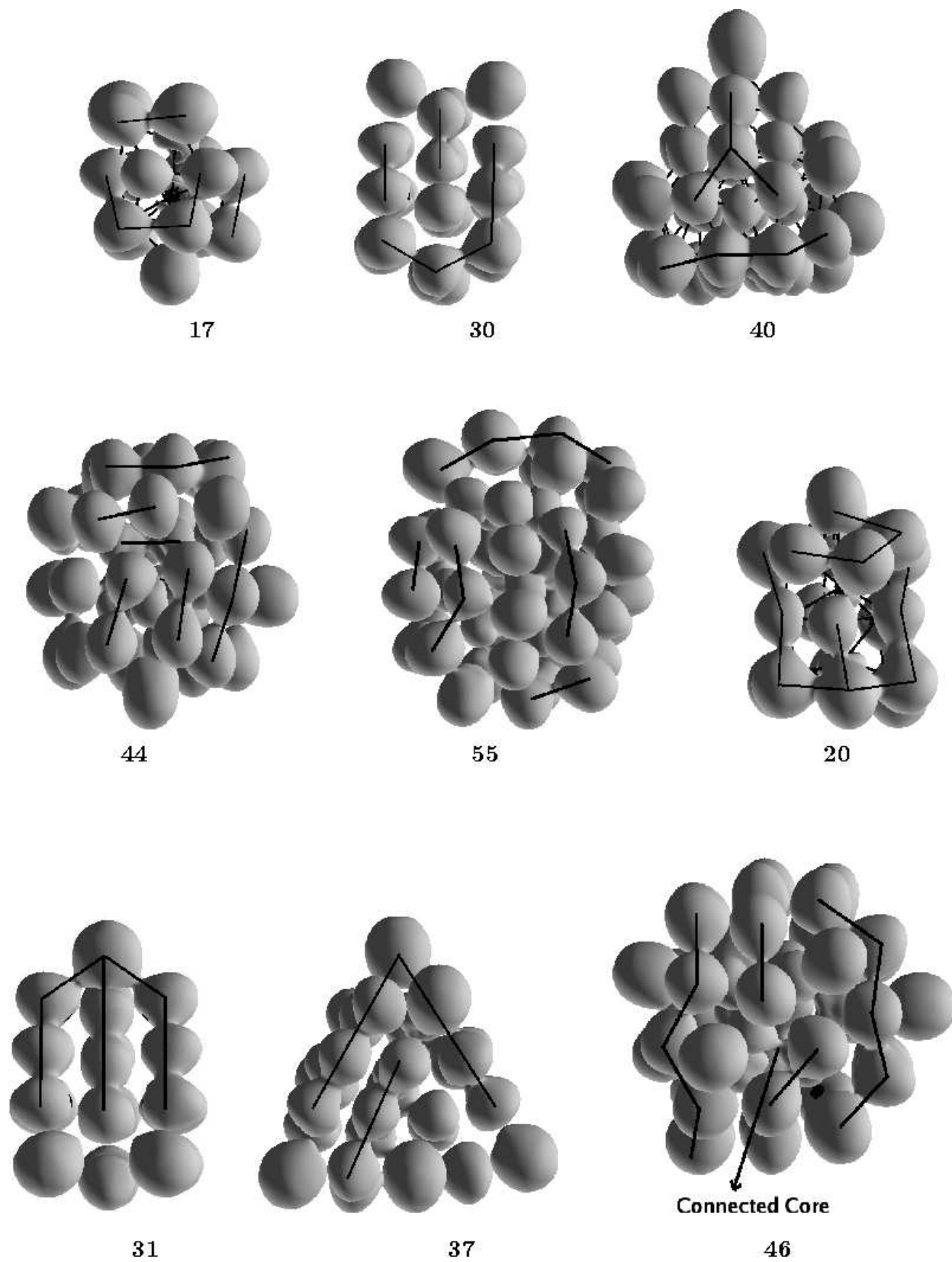


FIG. 6: Electron Localization Function (ELF) at an isovalue of 0.70 for various gallium clusters.

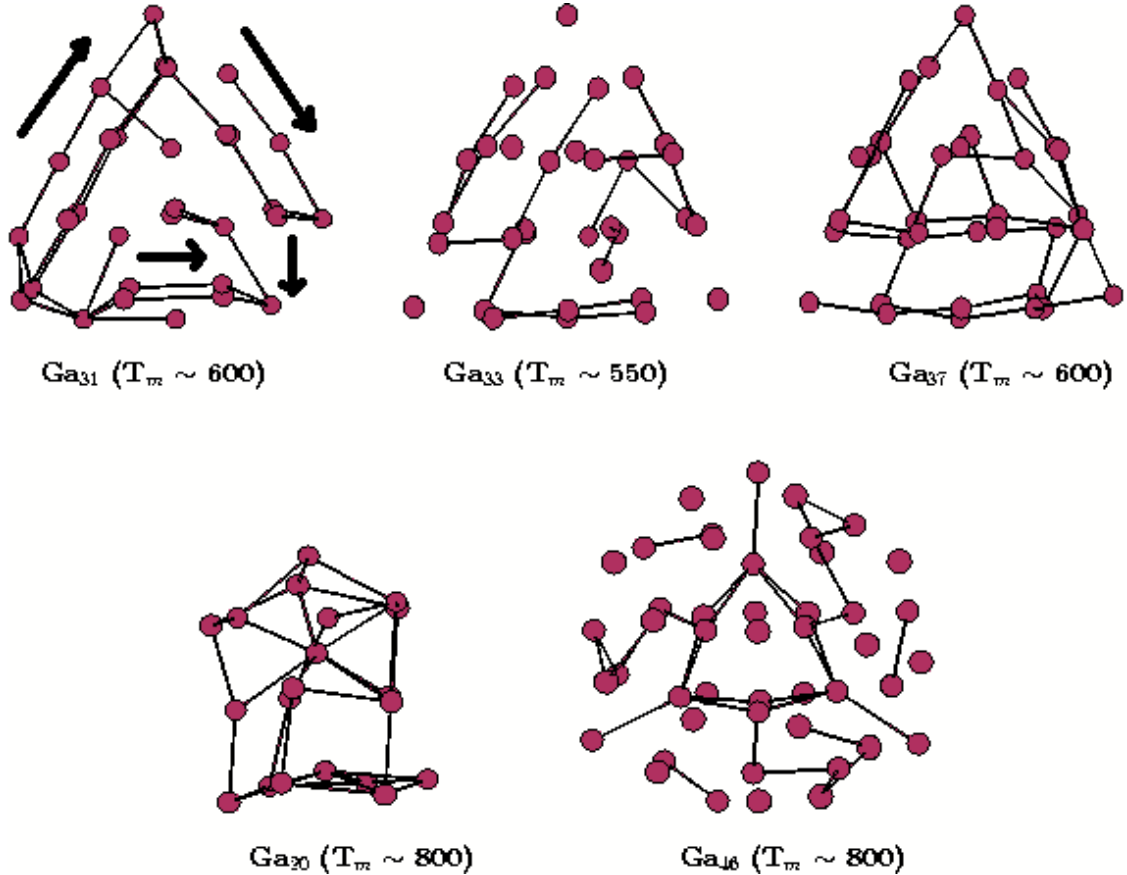


FIG. 7: Distribution of shortest bonds within the gallium clusters.

Therefore, we can expect the cluster to have a broad and continuous melting transition. Thus, our results confirm our earlier argument that there exists a definitive relationship between the local order in the cluster and its finite temperature behavior (and consequently the characteristics of the heat-capacity curve).<sup>11</sup>

We also show that as the cluster grows in size, it evolves through a succession of ordered and disordered geometries. In such cases an addition of one or few atoms changes the nature of the ground state geometry abruptly. The variation in the ground state results in the appearance or disappearance of the local order within the structure, leading to presence or absence of the melting peak, respectively. We now realize that this size sensitive nature of heat capacities is generic to small clusters and related to the evolutionary pattern seen in their ground states. The evidence for this comes not only from gallium clusters but also from clusters of sodium,<sup>14,23</sup> aluminum,<sup>24</sup> and gold<sup>15</sup> having very different nature of bonding.

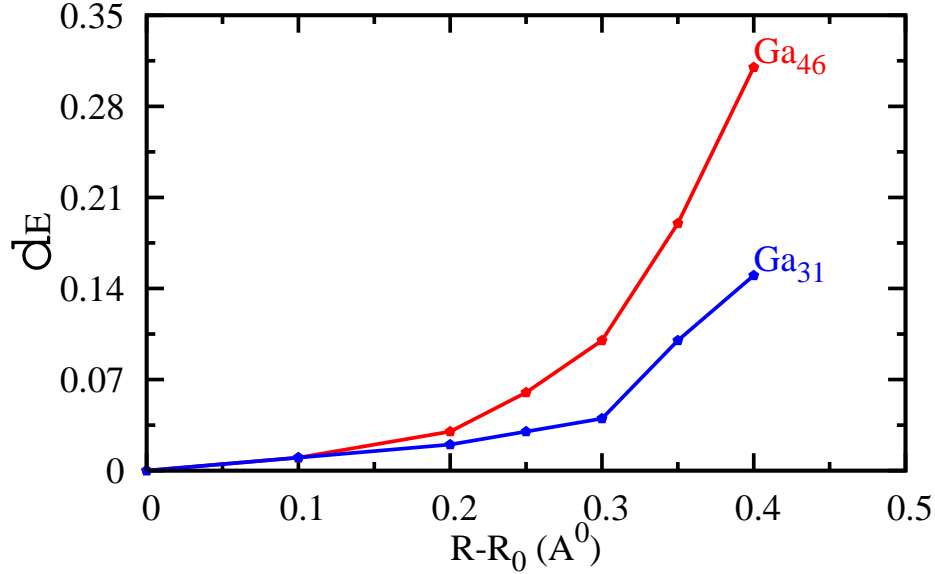


FIG. 8: Variation in the binding energy ( $d_E$ ) of cluster with respect to the displacement of surface atoms from their equilibrium positions ( $R_0$ ).

Next, we attempt to understand the reason behind the variations in the melting temperature in  $\text{Ga}_n$  ( $n = 20\text{--}46$ ) clusters. We analyze the structure and bonding of the clusters exhibiting a distinct melting transition viz.,  $\text{Ga}_{13}$ ,  $\text{Ga}_{20}$ ,  $\text{Ga}_{31}$ ,  $\text{Ga}_{33}$ ,  $\text{Ga}_{37}$ , and  $\text{Ga}_{46}$ . It may be recalled that  $\text{Ga}_{20}$  and  $\text{Ga}_{46}$  melt around 800 K, while  $\text{Ga}_{31}$ ,  $\text{Ga}_{33}$ , and  $\text{Ga}_{37}$  melt between 500–600 K. The first striking difference to note is the presence of core atoms in the  $\text{Ga}_{20}$  and  $\text{Ga}_{46}$  and absence of any distinct core in  $\text{Ga}_{31}$ ,  $\text{Ga}_{33}$ , and  $\text{Ga}_{37}$ . The distribution of the shortest bonds ( $\leq 2.70 \text{ \AA}$ ) in each cluster (which are also the atoms forming a single basin as indicated by ELF) is shown in Fig. 7. It is clearly noted that the shortest bonds in  $\text{Ga}_{20}$  and  $\text{Ga}_{46}$  are spread through out the cluster and more importantly they make a network connecting the core and the surface atoms. This results in a compact and stable electronic configuration in both the clusters as indicated by bunched eigen value spectrum as compared to evenly spread spectrum in case of all other clusters (figure not shown). On the other hand, in case of  $\text{Ga}_{31}$ ,  $\text{Ga}_{33}$ , and  $\text{Ga}_{37}$  the covalent bonds are restricted along the planes of the cluster. Thus, the pattern of bonding within these three clusters appears similar to that of pillared materials, where the atoms along the same plane are covalently bonded, while the bonds across the planes are weakly covalent or more metallic like in na-

ture. Hence, when these clusters are heated, the weaker inter-planar bonds are the first ones to break. This is followed by sliding of planes (constituting of equivalently bonded atoms) along each other. This argument correlates well with our analysis of ionic motion in  $\text{Ga}_{31}$ ,<sup>11</sup> where we see that as the cluster is heated, the planes begin to slide as shown by arrows in Fig. 7. This is initiated at a fairly lower temperature of 400 K. On further increase in the temperature of the cluster, the sliding planes collide against each other and the cluster melts around 600 K. On the other hand, the strong bonds between the core and surface atoms in  $\text{Ga}_{20}$  hold the surface atoms around their respective positions until a temperature of 600 K.<sup>12</sup> The cluster melts finally around 800 K. We further note that another cluster with a distinct core viz.,  $\text{Ga}_{13}$  also exhibits a network of strong covalent bonds between the core and surface atoms. Our earlier simulations indicate this cluster to melt at a relatively high temperature of 1300 K.<sup>10</sup>

Thus, we believe that the presence of a network of strong covalent bonds between the core and surface atoms results in greater stabilization of the surface atoms in  $\text{Ga}_{20}$  and  $\text{Ga}_{46}$ . These surface atoms therefore need to overcome a higher energy barrier to diffuse across the surface as compared to one in  $\text{Ga}_{31}$ ,  $\text{Ga}_{33}$ , and  $\text{Ga}_{37}$ . To demonstrate this, we stretch one of the atoms on the surface of  $\text{Ga}_{31}$  and  $\text{Ga}_{46}$ . This is done so as to mimic the motion of the atoms when the cluster is heated. The change in the binding energy of the cluster as function of the bond stretch is plotted in Fig. 7. It is easily noted from the figure that the surface atom of  $\text{Ga}_{46}$  requires more energy for displacement from its equilibrium position as compared to the one in  $\text{Ga}_{31}$ . This is true for most of the surface atoms of  $\text{Ga}_{46}$  and  $\text{Ga}_{31}$ . This analysis is also found to be similar in case of aluminum and sodium clusters. Our understanding is also in agreement with the results of Aguado and Lopez<sup>9</sup> for sodium clusters, where they have found a strong correlation between variation in  $T_m$  and core-surface distances.

#### IV. SUMMARY AND CONCLUSION

In the present work we have attempted to explain the reasons behind the characteristic features observed in the experimental heat capacity curves of gallium clusters in the size range of 20–55. As the gallium clusters grow, they are seen to pass through a cycle of spherical–prolate, prolate–oblate, and oblate–spherical transition. During the process they

pass through a succession of geometries with and without local “order” in bonding. It is the presence of a local “order” in the cluster that is responsible for the sharp peak in the heat capacity curve. Our studies also show that it is the presence of a distinct core and more importantly presence of a network of strong bonds between the core and surface atoms that is responsible for the higher melting temperature of the clusters.

## V. ACKNOWLEDGMENTS

We acknowledge the discussions and help received from Sharan Shetty during the search for ground state isomers. We acknowledge C-DAC(PUNE) for providing us with super-computing facilities. KJ and DGK thank Indo French Center For Promotion of Advanced Research (IFCPAR) for partial financial support (Project No. 3104-2).

- 
- <sup>1</sup> M. Schmidt, R. Kusche, W. Kronmuller, B. von Issendorff, and H. Haberland, *Phys. Rev. Lett.*, **79**, 99 (1997) ; M. Schmidt, R. Kusche, B. v. Issendorff, and H. Haberland, *Nature (London)*, **393**, 238 (1998).
  - <sup>2</sup> M. Schmidt and H. Haberland, *C. R. Physique*, **3**, 327 (2002).
  - <sup>3</sup> G. A. Breaux, R. C. Benirschke, T. Sugai, B. S. Kinnear, and M.F. Jarrold, *Phys. Rev. Lett.*, **91**, 215508 (2003).
  - <sup>4</sup> G. A. Breaux, D. A. Hillman, C. M. Neal, R. C. Benirschke, and M. F. Jarrold, *J. Am. Chem. Soc.*, **126**, 8628 (2004).
  - <sup>5</sup> G. A. Breaux, C. M. Neal, B. Cao, and M. F. Jarrold, *Phys. Rev. Lett.*, **94**, 173401 (2005).
  - <sup>6</sup> F. Calvo and F. Spiegelmann, *J. Chem. Phys.*, **112**, 2888 (2000); P. Blaise and S. A. Blundell, *Phys. Rev. B.*, **63**, 235409 (2001).
  - <sup>7</sup> A. Rytkönen, H. Häkkinen, and M. Manninen, *Phys. Rev. Lett.*, **80**, 3940 (1998); K. Manninen, H. Häkkinen, and M. Manninen, *Phys. Rev. A.*, **70**, 023203 (2004); K. Manninen, T. Santa-Nokki, H.äkkinen, and M. Manninen, *Eur. Phys. J. D.*, **34**, 43 (2005); A. Aguado, L. M. Molina, J. M. López, and J. A. Alonso, *Eur. Phys. J. D.*, **15**, 221 (2001).
  - <sup>8</sup> S. Chacko, D. G. Kanhere, and S. A. Blundell, *Phys. Rev. B.*, **71**, 155407 (2005).
  - <sup>9</sup> A. Aguado and J.M. Lopez, *Phys. Rev. Lett.*, **94**, 233401 (2005).

- <sup>10</sup> S. Chacko, K. Joshi, D. G. Kanhere, and S. A. Blundell, Phys. Rev. Lett., **92**, 135506 (2004).
- <sup>11</sup> K. Joshi, S. Krishnamurty, and D. G. Kanhere, Phys. Rev. Lett., **96**, 135703 (2006).
- <sup>12</sup> S. Krishnamurty, S. Chacko, D. G. Kanhere, G. A. Breaux, C. M. Neal, and M. F. Jarrold, Phys. Rev. B., **73**, 045406 (2006).
- <sup>13</sup> B. Song and P.L. Cao, J. Chem. Phys., **123**, 144312 (2005).
- <sup>14</sup> M-S. Lee and D. G. Kanhere, arXiv: cond-mat/0604281.
- <sup>15</sup> S. Ghazal, S. Krishnamurty, D. G. Kanhere, B. S. De Bas, and M. Ford, Manuscript under preperation.
- <sup>16</sup> X. G. Gong, G. L. Chiarotti, M. Parrinello, and E. Tosatti, Phys. Rev. B., **43**, 14277 (1991).
- <sup>17</sup> D. Vanderbilt, Phys. Rev. B., **41**, 7892 (1990).
- <sup>18</sup> Vienna *ab initio* simulation package, Technische Universität Wien (1999); G. Kresse and J. Furthmüller, Phys. Rev. B., **54**, 11169 (1996).
- <sup>19</sup> B. Silvi and A. Savin, Nature (London), **371**, 683 (1994).
- <sup>20</sup> J-Y. Yi, Phys. Rev. B., **61**, 7277 (2000).
- <sup>21</sup> R. Rousseau and D. Marx, Chem. Eur. J., **6**, 2982 (2000); *ibid*, Phys. Rev. Lett., **80**, 2574 (1998); *ibid*, J. Chem. Phys., **111**, 5091 (1999); *ibid*, Chem. Phys. Lett., **295**, 41 (1998).
- <sup>22</sup> A. D. Becke and K. E. Edgecombe, J. Chem. Phys., **92**, 5397 (1990).
- <sup>23</sup> M.S. Lee, S. Chacko, and D.G. Kanhere, J. Chem. Phys., **123**, 164310 (2005).
- <sup>24</sup> C. M. Neal, A. K. Starace, M. F. Jarrold, K. Joshi, S. Krishnamurty, and D.G. Kanhere, Unpublished results.